



Dye tracer aided investigation of xylem water transport velocity distributions

Stefan Seeger^{1,2} and Markus Weiler²

¹Soil Physics, Department of Crop Sciences, University of Göttingen

²Hydrology, Faculty of Environment and Natural Resources, University of Freiburg

Correspondence: Stefan Seeger (stefan.seeger@uni-goettingen.de)

Abstract. A vast majority of studies investigating the source depths in the soil of root water uptake with the help of water stable isotopes implicitly assumes that the isotopic signatures of root water uptake and xylem water are identical. In this study we show that this basic assumption is not necessarily valid, since water transport between the root tips and an observed point above the root zone is not instantaneous. However, to our knowledge no study has yet tried to explicitly assess the distribution of water transport velocities within the xylem. With a dye tracer experiment we could visualize how the transport of water through the xylem happens at a wide range of velocities which are distributed unequally throughout the xylem. In an additional virtual experiment we could show that, due to the unequal distribution of transport velocities throughout the xylem, different sampling approaches of water stable isotopes might effectively lead to xylem water samples with different underlying age distributions.

10 1 Introduction

Water stable isotopic signatures (δ^2H and $\delta^{18}O$) are a long established tool to study plant and root water uptake (Ehleringer and Dawson, 1992; Rothfuss and Javaux, 2017; Beyer et al., 2020) and transport. Since they are a part of the water molecule itself, they can be considered as ideal tracers to study soil-vegetation-atmosphere interactions. Additionally, in many regions of the world the isotopic composition of natural precipitation water exhibits a pronounced seasonality (Dansgaard, 1964; Rozanski et al., 1993). These naturally occurring fluctuations often lead to depth gradients of soil water isotopic signatures (δ_{soil}), which can be utilized to infer the contribution of different soil depths to root water uptake (RWU).

Rothfuss and Javaux (2017) reviewed 156 papers that investigated RWU with the help of stable water isotopes. They could be grouped into three categories: 46% of them were categorized as linear inference methods, 50% of them were isotopic mixing models and a mere 4% (seven in total) were numerical methods with a more process based conceptualization of RWU.

20 Irrespective of the chosen approach, all of the reviewed papers implicitly assumed an instantaneous equivalency between the isotopic signature in the soil and hence of RWU (δ_{RWU}) and the sampled isotopic signature of xylem water (δ_{xyl}).



1.1 Water storage and transport within the tree

Based on the observations of Meinzer et al. (2006), who applied deuterium labeling pulses to the bases of mature trees and traced them to twigs in the crown, Berry et al. (2018) reasoned that there is an *inherent time lag between water entering the root and reaching the xylem at the point of sampling*.

In order to account for this time lag, Magh et al. (2020) temporally shifted their soil isotopic data by constant tree specific time lags for *Fagus sylvatica* (European beech) and *Abies alba* (silver fir) trees before inferring potential water uptake source depths with a linear mixing model in a Bayesian framework (Parnell et al., 2013). The tree specific time lags were determined by dividing δ_{xyl} sampling heights through observed sap flow velocities (determined by sensors based on the heat ratio method).

De Deurwaerder et al. (2020) went a step further and developed the more dynamic mechanistic *SWIFT* (Stable Water Isotopic Fluctuation within Trees) model which consists of two parts: the first part computes RWU similar to the Feddes et al. (1976) RWU model depending on the water potentials in different soil depths and within the roots to predict δ_{RWU} (de Jong van Lier et al., 2008). Driven by fluctuating sap flow velocities, only the advective propagation of this δ_{RWU} signature along the trunk xylem is then simulated by the second part of the *SWIFT* model in order to predict δ_{xyl} at specific sampling heights.

Knighton et al. (2020) have tested a similar piston flow representation and a well mixed representation of plant internal water storage for *Fagus americana* (American beech) and *Tsuga canadensis* (Canadian hemlock) within the ecohydrological model *EcH2O-iso* (Kuppel et al., 2018). Both approaches improved the agreement between simulated and measured δ_{xyl} compared to the default model version with no consideration of tree internal water transport or storage.

Seeger and Weiler (2021) presented field data comprising 10 weeks of daily in-situ measurements of δ_{soil} in six depths and δ_{xyl} at three trunk heights of *Fagus sylvatica*. They estimated δ_{RWU} with a Feddes type RWU model after Jarvis (1989) and achieved a generally good agreement between those estimated δ_{RWU} values and observed δ_{xyl} measurements for (artificially labelled) 2H and (natural) ^{18}O signatures. However, they reported clear discrepancies between simulated δ_{RWU} and measured δ_{xyl} values in the wake of rapid δ_{RWU} changes. These discrepancies were largest for δ_{xyl} observations at 8m trunk height, but also clearly noticeable for δ_{xyl} observations at the base of the trunk. They utilized a convolution based transfer function approach to infer apparent flow path length distributions (FPLDs) between δ_{RWU} and δ_{xyl} . This led them to the conclusion, that the FPLD between root tips and trunk base is of a similar extent, but a different shape than the FPLD between trunk base and 8 m stem height. They did not manage to link the shape of the inferred transfer functions to any measurable characteristic of the studied trees.

Smith et al. (2022) adapted this transfer function approach for modelling the results of another in-situ isotope measurement study (Landgraf et al., 2022) on two *Salix* (Willow) trees with the ecohydrologic model *EcH2O-iso* (Kuppel et al., 2018). The parameters used to shape the transfer function have been determined via calibration and their final values were not reported or discussed. Compared to an instant mixing approach ($\delta_{RWU} = \delta_{xyl}$), the introduction of a transfer function between δ_{RWU} and δ_{xyl} did notably improve the agreement between simulated and observed δ_{xyl} values on a diurnal time scale, but not on a seasonal timescale.



Table 1. Combinations of sampling techniques (rows) and sampling domains (columns) that are discussed in this paper.

	Q	V_{mobile}	V_{total}	Core
Physiochemical extraction	✗	✗	✓	✓
In-situ equilibration	✗	✗	✗	✓
Transpiration capturing	✓	✗	✗	✗
Pressure extraction	✗	✓	✗	✗

55 While more recent scientific findings on the distribution of water transport velocities within tree xylem are either based on isotopic labeling (Kalma et al., 1998; James et al., 2003; Meinzer et al., 2006; Schwendenmann et al., 2010; Gaines et al., 2016) or thermometric methods (Čermák et al., 2004; Gebauer et al., 2008), approaches based on dye tracers have been used long before. Harvey (1930) reported on his use of *Light Green SF* as a fast penetrating and non-toxic dye to trace the flow paths of water through plant xylem. Subsequently, dye tracers have been used in a number of studies (Baker and James, 1933; Müller, 60 1949; Mathiesen, 1951) to investigate the velocity of the transpiration stream in *Acer pseudoplatanus* (sycamore), *Fagus sylvatica*, *Fraxinus excelsior* (European ash) and *Betula spec.* (birch). More recently, the much less destructive thermometric methods (Marshall, 1958; Granier, 1985) became the dominant approach to investigate sap flux velocities and the role of dye tracers was mainly reduced to a supplementary mean to determine conducting sapwood areas (Dawson, 1998; McJannet et al., 2007; Lubczynski et al., 2017).

65 1.2 Water pools captured by different sampling approaches

Methods to sample plant water for stable water isotope analyses can be grouped into four categories (rows of Tab. 1). Under *Physiochemical extractions* we subsume solvent based extraction techniques (Thorburn et al., 1993) and the nowadays much more common cryogenic vacuum distillation (Koeniger et al., 2011). The possible sampled water pools (columns of Tab. 1) for all of these methods do overlap more or less, but they are not identical:

70 Q : flux of water that is flowing through the cross sectional area of a stem xylem segment within a certain time span. Methods that capture the transpiration of individual plants (Kalma et al., 1998; Dubbert et al., 2014; Volkmann et al., 2016a; Kulmatiski and Forero, 2021) are effectively sampling from this water pool.

V_{total} : all water that is contained within a whole stem xylem segment. Physiochemical extraction applied to entire branch segments (Thorburn and Ehleringer, 1995; Zuecco et al., 2022) captures this water pool.

75 V_{mobile} : all mobile water that is contained within a whole stem xylem segment. This water pool can be sampled with a Scholander pressure chamber (Geißler et al., 2019; Magh et al., 2020; Zuecco et al., 2022) or a cavitron flow-rotor (Barbeta et al., 2022).

Core: all water contained within a xylem core sample. δ_{xy1} of such core samples can be obtained by physiochemical extraction (Dawson and Ehleringer, 1991), nowadays mostly CVD (Koeniger et al., 2011; Kahmen et al., 2021; Snelgrove et al.,



80 2021; Fabiani et al., 2022). A similar domain is sampled by in-situ vapor equilibration approaches based on either probes (Volkman et al., 2016b; Seeger and Weiler, 2021; Menekes et al., 2021; Gessler et al., 2022) or boreholes through the whole stem (Marshall et al., 2020; Landgraf et al., 2022; Kühnhammer et al., 2022).

1.3 Study objectives

Since water has to be transported from one point in the xylem to another and this transport is by no means instantaneous, we should not assume that δ_{RWU} is directly reflected by measurements of δ_{xy1} at the same point in time. While several isotopic labeling studies have shown that δ_{xy1} between two different points in the xylem are different due to transformative effects of xylem water transport, no study has yet tried to explicitly assess the distribution of tracer transport velocities within the xylem. The primary objective of this study was to test whether an inexpensive dye tracer approach can be used to chart the distribution of water transport velocities within tree xylem. The secondary objective of this study was to compare the underlying water transport velocity distributions associated to different δ_{xy1} sampling approaches.

2 Methods

2.1 Dye tracer experiment

2.1.1 Experimental setup

In order to visualize the distribution of tracer transport velocities within tree xylem, we conducted a dye tracer experiment whose setup is illustrated in Fig. 1 and which will be described in the following section.

We selected a 95 cm long stem segment (diameter of 3.5 cm) of a young *Salix* (willow) tree. The stem segment was harvested shortly before leaf-out in April 2022 from a garden on drained Gleysol in the municipality of Ihringen, Southwestern Germany (48°3'N 7°39'E, 190 m a.s.l.). There is no inherent importance of the species, size or provenience of the selected specimen, it only serves as an example to test the presented method.

100 Between sampling the stem segment and the start of the experiment (approximately 24 hours), we wrapped both ends of the stem segment in wet towels covered by plastic bags to avoid cavitation. Shortly before the start of the experiment, we cut another 5 cm of both ends of the stem segment. Subsequently, the stem segment was fixed to a rig, upside-down compared to its original orientation. A large funnel was placed on top of it. The base of the stem segment was connected to the outlet of the funnel with a piece of bicycle tubing and hose clamps. Below the stem segment, we placed a beaker that collected all water dripping out of the stem segment (Fig. 1a). Initially, we filled the funnel with tap water and waited for a few minutes to ensure that we have a steady flow of water through the stem segment. Then, we emptied the funnel and the beaker and filled the former one with 4 litres of dye infused tap water (4g/L Brilliant blue FCF). As soon as the first visible dyed drop of water left the stem segment, we removed the stem segment from the rig and placed it horizontally to stop the gravitation driven water flow. Then we used a band-saw to cut the stem segments into approximately 5 cm long sub-segments (Fig. 1b). After measuring the segments' diameters and lengths, they were placed next to each other and photographed (Fig. 1c).

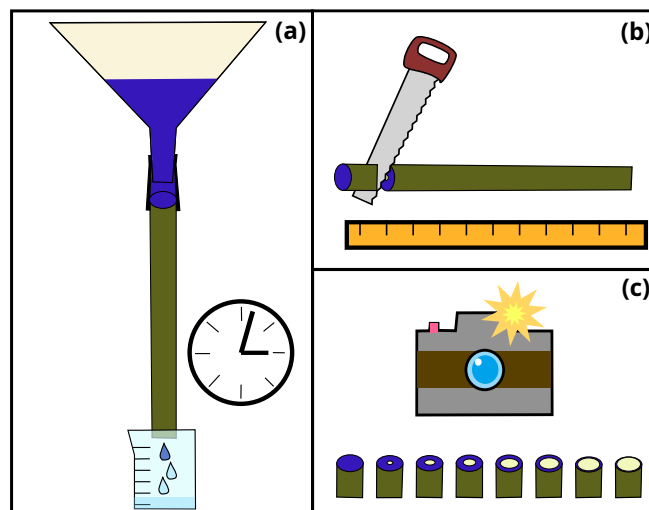


Figure 1. Sketch to illustrate the steps of the dye tracer experiment: (a) Application of dye tracer to stem segment; (b) Cutting the stem into smaller sub-segments; (c) Capturing images of cut surfaces for each sub-segment

2.1.2 Data processing

We used the image processing software ImageJ (Schneider et al., 2012) to manually crop each of the stem sub-segments out of the captured image and stored them in separate image files (Fig.2a). We then used ImageJ to manually create masks that indicate the xylem (excluding image background, bark and phloem) of each sub-segment and stored them in another set of files

115 (Fig.2b).

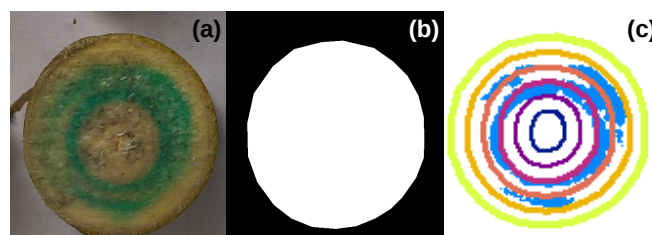


Figure 2. Exemplary images for the image processing of cut surface #15. (a) shows the original photograph, (b) is the respective xylem mask and (c) shows the detected blue stained area (light blue pixels) within six xylem depth classes (outer borders depicted by dark blue to yellow circles)

With the cropped image files of each stem sub-segment and the respective masks, we automated the further data processing within the R-software environment (RCoreTeam, 2022) where we used the package *readbitmap* (Jefferis, 2018) to load the image files and their respective xylem masks. Apart from excluding non xylem pixels from the automated analysis, the xylem masks



were also used to determine the distance of each xylem pixel to the nearest non xylem pixel. These xylem border distances
120 were then used to assign each pixel to one of six xylem depth classes.

In order to automatically decide whether a xylem pixel should be counted as stained from the blue dye tracer, we adapted the formula used to determine the NDVI (normalized difference vegetation index (Tucker, 1979; Hayes, 1985)) and computed a "normalized difference blueness index" (NDBI), based on the blue (B) and red (R) RGB values of each pixel:

$$\text{NDBI} = \frac{B - R}{B + R} \quad (1)$$

125 Based on our own visual comparisons, we classified pixels with an $\text{NDBI} < -0.05$ as unstained and those with $\text{NDBI} \geq -0.05$ as stained (Fig.2c). Based on this classification, we determined the fractions of blue stained area (F) for cut surface n and xylem depth class d as:

$$F_{n,d} = S_{n,d}/A_n \quad (2)$$

where A_n is the number of all pixels in the respective cut surface's xylem mask and $S_{n,d}$ is the number of stained pixels within
130 xylem depth class d . Subsequently we determined the differences in stained area fractions between adjacent cut surfaces for each depth class with:

$$f_{n,d} = F_{n-1,d} - F_{n,d} \quad (3)$$

where $F_{n-1,d}$ belongs to the cut surface closer to the stem base. Finally, we computed the required velocities to reach each cut surface within the tracer application time t with the simple equation:

135 $u_n = s_n/t$ (4)

where s_n is the distance between the stem base and the original position of the n^{th} cut surface. The combination of $f_{n,d}$ and u_n represents velocity density distributions for different xylem depths whose resolution is given by the number of cut surfaces. The mean tracer transport velocity within each depth class d could then be computed as:

$$\bar{u}_d = \frac{\sum_{n=1}^N (f_{n,d} \times u_n)}{\sum_{n=1}^N f_{n,d}} \quad (5)$$

140 where N is the total number off all cut surfaces. The overall transport velocity \bar{u} is computed similarly as an area weighted mean of all \bar{u}_n values.

Complementarily, we also computed q , the volumetric flux of water through the whole stem segment:

$$q = \frac{Q}{A} = \frac{V}{At} \quad (6)$$

where A a is the cross sectional area of the stem segment and Q the discharge, which is equal to V (the volume of water which
145 dripped into the beaker) divided by the respective duration t .



2.2 Velocity distributions of water samples captured by different sampling approaches

Water samples taken from a xylem segment may capture different water velocity distributions depending on the applied sampling approach. In a virtual experiment we first generated a hypothetical xylem segment with a known idealized distribution of water transport velocities and then we compared the effective velocity distributions that would be captured by five different sampling approaches.

2.2.1 Generation of virtual xylem segment with idealized transport velocity distribution

The absolute dimension of our hypothetical xylem segment (depicted in Fig. 3a) does not matter, but it is characterized by an idealized distribution of tracer transport velocities similar to the observations made with the dye tracer experiment. We conceptualized the xylem segment with $D (= 12)$ equally spaced xylem depth classes. Possible transport velocities were discretized in N steps reaching from $u_0 = 0$ to $u_N = u_{max}$. Now the frequency density matrix $f_{n,d}^*$ (with n in $[0, \dots, N]$ and d in $[1, \dots, D]$) can be used to describe the frequencies of certain velocities at certain xylem depth classes. This depth class specific velocity density distribution described by $f_{n,d}^*$ can be transformed into the xylem wide velocity density distribution $f_{n,d}$ (see Eq. 3), by weighing the densities of each depth class with the respective depth class' area fraction of the total cross sectional area.

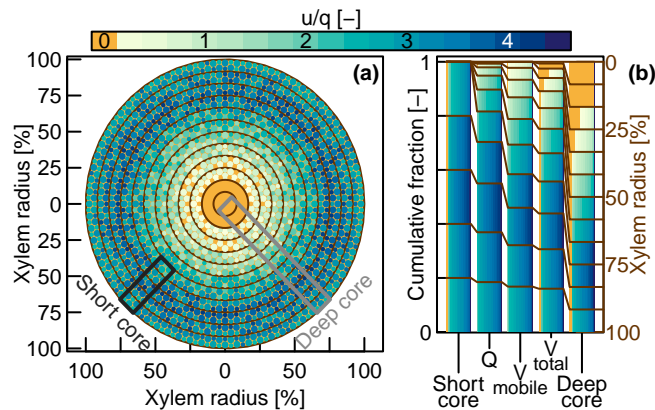


Figure 3. (a) Conceptual velocity distribution within a xylem cross section. Transport velocity distributions of mobile water within each depth class are depicted by four kinds of tiny circles. Each circle's color corresponds to the mean velocity of a certain quantile range between the 0.15, 0.5, 0.85 and 1 quantiles of the velocity distribution. The circles' areas correspond to the respective quantile ranges' sizes. (b) Compositions of effective velocity distributions associated to hypothetical water samples acquired by different sampling approaches.

In order to fill $f_{n,d}^*$, we iterated over all xylem depth classes (d between 1 and D), and determined the frequencies of certain velocities by computing a Gaussian density distribution with a standard deviation of σ_d around the respective depth class' mean velocity \bar{u}_d . Values for \bar{u}_d were set to 0 for the two innermost depth classes, steadily incremented towards their highest value (u_{max}) shortly before the outer xylem and then slightly decreased at outer most xylem. The described values for \bar{u}_d and the



values of σ_d ($0u_{max}$ for $d \leq 2$ and $0.08u_{max}$ for $d > 2$) were selected in order to achieve an idealized velocity distribution
165 similar to the observations of the dye tracer experiment. Finally, we added an immobile water fraction $\phi_i = 0.1$ to all depth
classes where $\bar{u}_d > 0$ (all but the two innermost depth classes) according to the following equation:

$$f_{0,d}^* = \frac{\sum_{n=1}^N f_{n,d}^*}{\phi_i^{-1} - 1} \quad (7)$$

This immobile water fraction is meant to account for water that might influence δ_{xy1} measurements while it is not actively
participating in the transport of water through the xylem. The value of 10% was chosen rather arbitrarily since we could not
170 find any studies that reported the ratio of mobile to immobile water within tree xylem.

2.2.2 Virtual sampling

At that point, $f_{n,d}^*$ represented the information about the frequencies of specific velocities at specific depth classes within
the xylem. Different sampling approaches would capture different parts and/or proportions of this original $f_{n,d}^*$. For a virtual
method inter comparison we considered the four approaches described in Sec. 1.2, but split the *Core* case into *Deep core*
175 (spanning the whole xylem depth) and *Short core* (limited to the outer five xylem depth classes as depicted in Fig.3a):

- Q : $f_{n,d}^*$ is weighted by A_d (area of each xylem depth class d) and u_n (velocity of each velocity class n).
- V_{total} : $f_{n,d}^*$ is weighted by A_d .
- V_{mobile} : $f_{n,d}^*$ (with $n \geq 1$) is weighted by A_d . $f_{0,d}^*$ (the fraction of immobile water across all depth classes) is set to 0.
- Deep core: $f_{n,d}^*$ is taken as it is.
- 180 – Short core: $f_{n,d}^*$ is taken as it is, but all values where $d \leq (D - 5)$ are set to 0.

3 Results

3.1 Transport velocities within the xylem

With the timer starting at the first application of the dye tracer, it took 42 minutes until the first drops containing a visually
detectable amount of blue dye tracer dropped into the beaker placed under the stem segment. Within that time, 140 mL of
185 water were collected in the beaker. With a xylem diameter of 32.5 mm (measured at the thinner end of the stem segment), the
cross sectional area amounted to 8.3 cm². Consequently, the flux of water through the stem segment was 5.7 md⁻¹.

Even though there had been some visibly dyed water dropping out of the stem segment, cut surface #18, farthest away from
the tracer injection point, did not show any visible traces of the dye tracer. Figure 4a shows digitized images of the stem segment
cut-surfaces. Pixels with NDBI values above the threshold of -0.05 are depicted blue. The colored contour lines (yellow to dark
190 blue) indicate the outer extents of six automatically delineated xylem depth classes. Figure 4b shows the fractions of dye
stained area grouped by the respective xylem depth classes. Starting with close to 100% dye stained area at the first cut surface



(which was directly exposed to the dye tracer at the outlet of the funnel), the stained area fraction diminished quickest at the innermost xylem depth class and the second innermost depth class. For the cut surfaces #1-9, the fraction of stained area of the four outer depth classes remained virtually constant at around 85%. After that, the stained area fractions decreased for all depth classes. The outermost depth class showed no more dye stains after 65 cm (cut surface #14). The second outermost depth class was most persistent, still showing dye traces up to the penultimate cut surface #17.

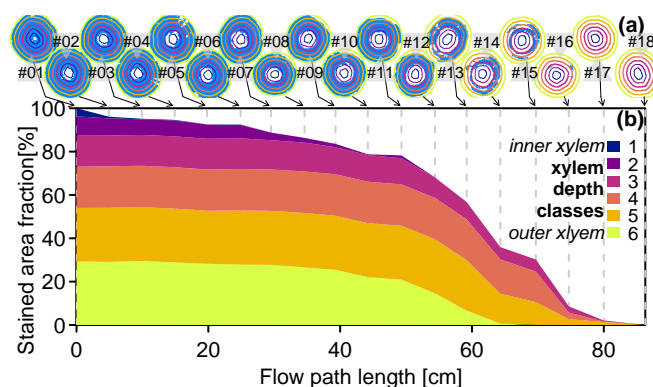


Figure 4. (a) Digitized cut surfaces with stained areas, overlain with outer extents of xylem depth classes (yellow to dark blue lines). (b) Cumulated stained area fractions by xylem depth class.

The dye tracer transport velocity distribution for the whole stem is represented by the stacked colored areas in Fig. 5a. With a value of $5.7 \text{ m}^1 d^{-1}$, the xylem water flux velocity q (computed with Eq. 2.1.2) was less than a third of the mean tracer transport velocity \bar{u} with a value of $17.4 \text{ m}^1 d^{-1}$ and about one fifth of the highest tracer velocity of $28 \text{ m}^1 d^{-1}$, which was observed at the 3rd, 4th and 5th xylem depth class.

Figure 5b depicts the individual tracer transport velocity distributions for the six xylem depth classes. The velocity distributions for the outer three depth classes resembled a normal distribution, while the third depth class featured a skewed and multimodal velocity distribution. The tracer velocity distribution of the inner most xylem depth class had a clear peak at $0 \text{ m}^1 d^{-1}$. Complimentary, Fig. 5c shows the tracer velocity distributions plotted against the xylem depth. Tracer velocities were increasing from the xylem center to the outer xylem, peaking at around 60% of the xylem radius and then slightly decreased towards the outer xylem.

3.2 Transport velocity distributions captured by different sampling approaches

The transport velocity distributions (TVDs) of water samples captured by different hypothetical sampling approaches for one and the same xylem segment are shown in Fig. 6a-e. For reference purposes, the TVD of the xylem water flow (TVD_Q) was plotted as a grey area into each of the TVD plots shown in Fig 6 and all velocities were given as multiples of the volumetric flux q . While the mean transport velocities (\bar{u} , dashed vertical black lines in Fig. 6) ranged from $1.7q$ (Fig. 6d) to $3q$ (Fig. 6a), the highest captured transport velocity was the same for all sampling approaches. The TVD for the sampling of mobile

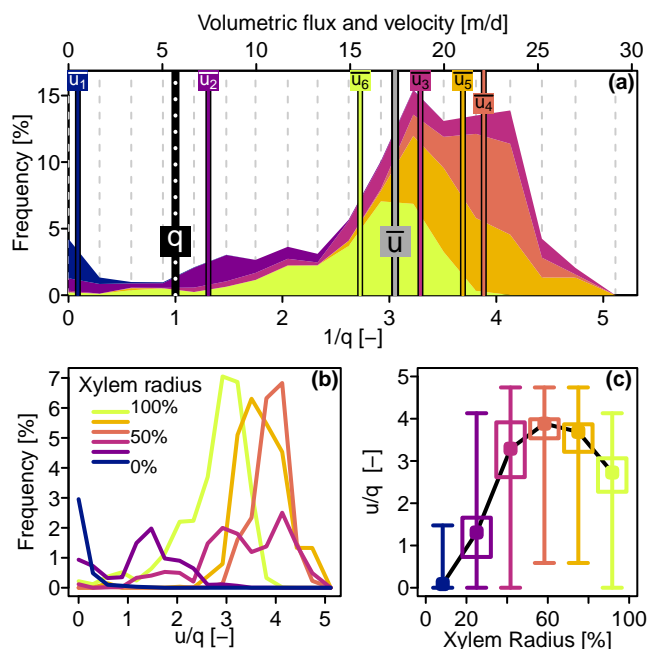


Figure 5. (a) Stacked colored areas show the contributions of six xylem depth classes (inner xylem = dark blue, outer xylem = yellow) to the overall tracer transport velocity distribution. Vertical bars indicate mean transport velocities per depth class (\bar{u}_1 to \bar{u}_6), overall mean transport velocity \bar{u} and volumetric flux q . (b) Tracer transport velocity distributions for the individual xylem depth classes. (c) Tracer transport velocities plotted against xylem depth – whiskers indicate depth classes’ absolute ranges, boxes the 25-75 % quantile ranges and points the mean values.

water (Fig. 6b) was most similar to TVD_Q , even though the outer xylem was slightly under- and the inner xylem slightly over represented. The short core’s TVD (Fig. 6e), which completely excluded the inner xylem, was surprisingly similar to TVD_Q , while the deep core’s TVD (Fig. 6d) showed the least resemblance to TVD_Q due to a strong over representation of the much less mobile inner xylem water. While the TVDs of the xylem water flow and the mobile water volume (Fig.6a&b) were not influenced by immobile water, the other three cases (Fig.6c-e) contained immobile water fractions between 10 and 29%. The latter maximum value was reached from the deep core sampling scenario, which sampled all xylem depths classes to equal parts and thereby incorporated a disproportionately high fraction of the innermost xylem, which is not actively taking part in the water transport.

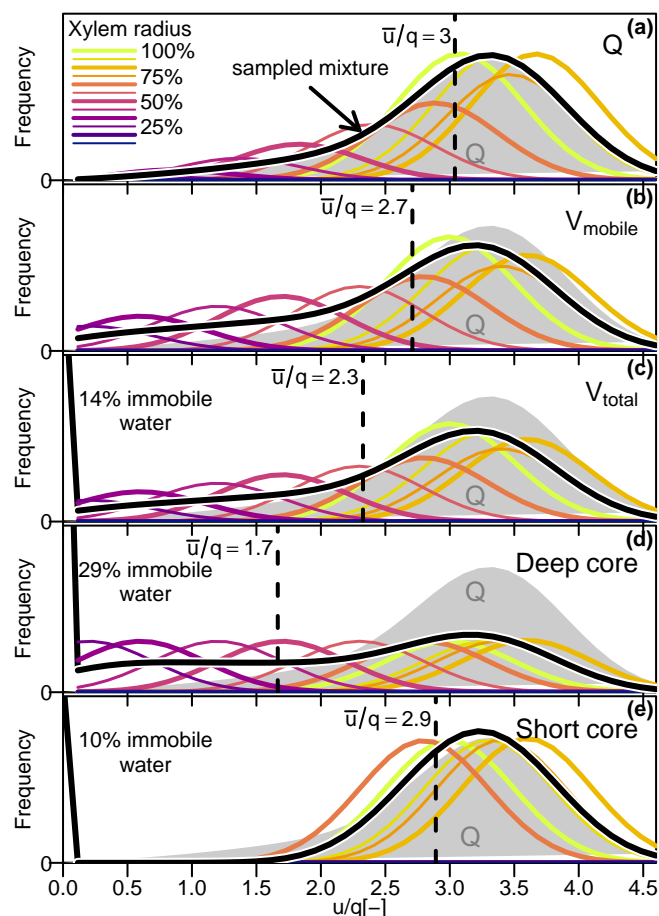


Figure 6. Tracer transport velocity distributions captured by a sample (thick black line) and the contributions of different xylem depths (colored lines, scaled by 400%) for different sampling approaches. (a) Actual throughflow, (b) Mobile water volume, (c) Total water volume, (d) Deep core, (e) Short core.

4 Discussion

4.1 Dye tracer experiment

In order to make full use of the potential of the proposed method to infer tracer velocity distributions within the xylem, several aspects of the lab experiment introduced in this study could be improved.

225 The general purpose band-saw that we used to cut the stem into sub-segments produced rather rough cut surfaces and occasionally left some grime. At the time of the image capturing, some of the sub-segments' cut-surfaces were partially covered by saw dust. This could be improved by using a cleaner and finer wood saw and more thorough post-treatment of the cut-surfaces (e.g. blasting them with pressurized air or sanding).



Another consideration would be a more controlled way to take the images. We placed all 18 sub-segments next to each other
230 and photographed all of them at once under ambient light. This lead to a) optical distortion of the segments placed off the
center of the image and b) non-uniform lighting conditions. Photographing each segment individually directly from above and
at a constant distance under well lit conditions could greatly reduce optical distortions and would enable a more quantitative
evaluation of the dye patterns by accounting for the staining intensity instead of just classifying into stained/unstained areas.
On top of that, it might be much easier to automatically process these images and it might eliminate the need for the manual
235 steps of cropping the individual segments and creating xylem masks. In the best case, it might even be possible to automate the
identification of single year rings and get rid of the rather arbitrary depth class zoning.

However, there is a certain limit to the time that can be spent to post-process and photograph the stem segments. Twelve
hours of storage of the sub-segments at room temperature (exposed to the atmosphere) lead to evaporation from the cut-surface
which caused additional water and dye tracer movement, completely confounding the patterns we were interested in. We
240 managed to capture the patterns quickly (all 18 sub-segments were cut and captured within one image in about 10 minutes),
but more thorough post-processing and imaging might require special measures to reduce post-cut evaporation. Umebayashi
et al. (2007) reported that immersion in liquid nitrogen and subsequent freeze drying of fresh cut xylem conserved the dye
distribution at cutting time and allowed for more elaborate post processing steps like slicing with a microtome.

4.2 Tracer velocity distributions within the xylem

245 Even though a comparison between the highest transport velocities observed in our dye tracer experiment and those (implicit-
ly) reported in the studies of Baker and James (1933), Müller (1949) and Mathiesen (1951) would be possible, it would be
problematic. In our study we applied a nearly constant positive water potential (starting the experiment with 4 L of water in the
funnel atop the stem base and ending it with 3.86 L, while the aforementioned studies all worked with the not further specified
natural transpiration stream (influenced by undocumented environmental conditions like radiation, wind speed, air humidity
250 and temperature), which can be expected to vary during and differ between single experiments conducted at different times and
locations.

Instead of looking at specific velocities, it might be more helpful, to focus on the observed ratio of maximum transport
velocity to the observed volumetric flux. Our dye tracing experiment suggested that the fastest tracer transport velocities (u_{\max})
were about 5 times as fast than the mean volumetric flux q . Other dye tracer studies did not report the respective volumetric
255 fluxes, but several studies that traced the propagation of a D_2O pulse injected to the base of the trunk of trees up to the leaves
(Meinzer et al., 2006; Schwendenmann et al., 2010; Gaines et al., 2016) have reported maximum tracer velocities to be about
4 to 16 times faster than mean sap flux velocities. Seeger and Weiler (2021) observed a deuterium labeling pulse passing at
two in-situ xylem water isotope probes installed at 0.1 and 8 m height also observed that maximum tracer transport velocities
and sap flux velocities differ by a factor of 5.5. Mennekes et al. (2021) reported tracer velocities much closer to the observed
260 sap flux velocities, but the investigated trees were comparatively small and the distances may have been too short in relation to
 δ_{xyl} observation frequencies to actually capture the fastest fraction of the tracer signal.



265 Although the *Brilliant Blue FCF* dye tracer used in this study has a larger molecular structure than the water itself, its application within a cut stem led to observations in good agreement with isotope based studies. Nevertheless, a direct comparison between the breakthrough curves of stable water isotopes and different dye tracers would be interesting and could increase the confidence in the validity of the approach of this study.

270 With regard to the depth distribution of tracer transport velocities, the study of Müller (1949) reports the highest transport velocities to occur in the outermost two year rings of *Fagus sylvatica* and a steady decline of transport velocities towards the inner xylem, with still detectable dye tracer transport up to the 24th youngest year ring of a 40 year old tree. Gebauer et al. (2008), who used thermoelectric sap flux sensors at different xylem depths to infer radial velocity distributions for sap flux, reported a similar pattern for the sap flux velocities of *Fagus sylvatica* (European beech), but for *Acer pseudoplatanus* (sycamore maple), *Acer campestre* (field maple), *Carpinus betulus* (hornbeam) and *Tilia spec.* (linden) they observed a pattern similar to the one observed in this study, with a velocity maximum close to the outer xylem but a slight velocity drop towards the outermost xylem. Čermák et al. (2008) reported the same radial velocity distribution for sap flux velocities of *Pinus sylvestris* (Scots pine).

275 It should be noted that with the presented experimental setup we were solely looking at one specimen of one tree species at one particular boundary condition provided by a nearly constant and uniform water potential applied to the base of the stem segment. Čermák et al. (2008) observed changes in the sap flux velocity distribution over xylem depth of *Pinus sylvestris* with decreasing top soil water availability. This lead to a notable decrease of sap flux velocity in the outer xylem (connected to rather shallow lateral roots) while sap flux in the inner xylem (connected to deeper roots) was maintained at a level close to the pre-drought conditions. Consequently, it might be better to interpret the results of our dye tracing experiment as a conductivity distribution instead of a velocity distribution. Only at uniform water potentials across the whole radial xylem depth range the two distributions can be expected to be congruent.

285 The dye tracer experiment presented in this study was performed on a diffuse porous angiosperm tree species, of which there are a lot more, very common trees. However, there are also many ring porous angiosperm genera like *Quercus* (oak), *Castanea* (chestnut), *Fraxinus* (ash), *Ulmus* (elm) and *Juglans* (walnut) which feature a completely different xylem structure with much fewer but far bigger and more conductive pores. The xylem structure of another big group of trees, the gymnosperms (mainly conifers) also differs markedly from diffuse porous trees. it is very likely that anatomically differing kinds of xylem will behave quite different in terms of water transport (Steppe and Lemeur, 2007). Therefore we would highly recommend to include ring porous trees and conifers into future investigations of xylem tracer transport velocity distributions.

290 4.3 Velocity distributions captured by different sampling approaches

Considering the differences between the waters that are sampled by the various discussed sampling approaches, it is reassuring to see that there are multiple approaches which do not dramatically deviate from the xylem water flow Q , which is probably closest to what we actually intend to measure. However, it would be helpful to further investigate whether a sampling approach similar to the *Deep core* case is actually as delayed compared to the xylem water flow due to an over representation of slow and



295 immobile water as it may seem from our results. Depending on the question at hand, it might be advisable to choose another
sampling approach, especially when temporal variability can be expected to play a role.

We also have to acknowledge that the immobile water fraction of 10% within conducting xylem depths in our virtual
comparison experiment was just an arbitrary assumption, which might be worthwhile to scrutinize in real world experiments.
Real world comparisons of different approaches are rare (Volkman et al., 2016b; Menekes et al., 2021; Zuecco et al., 2022)
300 and so far have not been conducted with sufficient temporal resolution to compare temporal dynamics of different approaches.
On top of that, other issues related to the differences between sampling approaches themselves, as discussed by Millar et al.
(2022), may cause bigger discrepancies than mere differences in the temporal dynamics of the captured water pools.

4.4 Implications for stable water isotope aided investigations of RWU

Our dye tracer experiment showed that water transport within the xylem is happening at a wide range of velocities. This means,
305 that the propagation of isotopic signatures through the xylem cannot be properly represented by a simple piston flow model
like previously attempted by De Deurwaerder et al. (2020); Knighton et al. (2020) and Magh et al. (2020). Moreover, since
even within the conducting sapwood only a certain fraction of the xylem is contributing to the water transport, the mean tracer
transport velocity can be expected to be higher than the mean sap flux velocity (in our case it was around three times as fast).
Maximum tracer transport velocities are even higher (in our case five times as fast as the mean sap flux velocity). As the
310 xylem water is transported at different velocities, abrupt changes of δ_{xyl} at the base of the stem will be blurred along their
way towards the crown. This means, that δ_{xyl} measurements close to the stem base will be more similar to actual δ_{RWU} . But
since RWU is happening at various points throughout the root system, even δ_{xyl} measurements right at the stem base are not
necessarily reflecting current δ_{RWU} (Seeger and Weiler, 2021). Instead, δ_{RWU} signals are blurred by a combination of the the
TVDs within the root xylem and different flow path lengths (due to the spatial organization of the root system) before they
315 even reach the stem base.

Current review studies (Dubbert et al., 2023) acknowledge a certain relevance to plant internal water travel times but at they
also state that the current understanding of them is limited. We think, that investigations of RWU that use δ_{xyl} measurements
should aim for a correct representation of the relationship between δ_{RWU} and δ_{xyl} . TVDs within the xylem are an essential
component of this relationship. They should be studied systematically in order to improve process based plant water uptake
320 modeling.

5 Conclusions

In this paper, we presented an inexpensive approach to assess xylem internal water transport velocity distributions and we
found a wide range of transport velocities within the xylem with a mean and maximum velocity of 300% and 500% of the
volumetric water flux, respectively. Velocity distributions at certain xylem depths tended to be normal distributed around mean
325 values which decreased towards the inner xylem.



By means of a theoretical assessment of the water transport velocity distributions associated to different xylem water sampling approaches, we found that most approaches sample water with specific underlying velocity distributions similar to that of the actual throughflow of xylem water. A notable exception would be comparatively deep cores from thin stems, which might capture disproportionately high fractions of very slow and immobile water.

330 The common assumption of an equivalency between δ_{RWU} and δ_{xy1} is a simplification. Water that is taken up at a specific point in time cannot be sampled from the xylem - neither at that specific point in time nor with a certain delay. Measurements of δ_{xy1} will always be composed of a mixture of waters taken up at different points in the past. In case of low δ_{RWU} variability or comparatively high transport velocities, the effects described in this paper may be negligible, but especially for the correct interpretation of high-frequency δ_{xy1} observations such water transport velocity distributions should be kept in mind.

335 *Author contributions.* SS planned, executed and analysed the dye tracer experiment, conducted all computations and wrote the first draft of the manuscript. MW participated in the discussion and helped to complete the manuscript.

Competing interests. Markus Weiler is editor of HESS

Acknowledgements. We would like to thank Annette Bösmeier for her assistance during the dye-tracer experiment and Natalie Orłowski for her constructive review of the manuscript.



340 References

- Baker, H. and James, W. O.: The Behaviour of Dyes in the Transpiration Stream of Sycamores (*Acer Pseudoplatanus* L.), *New Phytologist*, 32, 245–260, <https://doi.org/10.1111/j.1469-8137.1933.tb07010.x>, 1933.
- Barbeta, A., Burlett, R., Martín-Gómez, P., Fréjaville, B., Devert, N., Wingate, L., Domec, J.-C., and Ogée, J.: Evidence for Distinct Isotopic Compositions of Sap and Tissue Water in Tree Stems: Consequences for Plant Water Source Identification, *New Phytologist*, 233, 1121–1132, <https://doi.org/10.1111/nph.17857>, 2022.
- 345 Berry, Z. C., Evaristo, J., Moore, G., Poca, M., Steppe, K., Verrot, L., Asbjornsen, H., Borma, L. S., Bretfeld, M., Hervé-Fernández, P., Seyfried, M., Schwendenmann, L., Sinacore, K., De Wispelaere, L., and McDonnell, J.: The Two Water Worlds Hypothesis: Addressing Multiple Working Hypotheses and Proposing a Way Forward, *Ecohydrology*, 11, e1843, <https://doi.org/10.1002/eco.1843>, 2018.
- Beyer, M., Kühnhammer, K., and Dubbert, M.: In Situ Measurements of Soil and Plant Water Isotopes: A Review of Approaches, Practical Considerations and a Vision for the Future, *Hydrology and Earth System Sciences*, 24, 4413–4440, <https://doi.org/10.5194/hess-24-4413-2020>, 2020.
- 350 Čermák, J., Kučera, J., and Nadezhkina, N.: Sap Flow Measurements with Some Thermodynamic Methods, Flow Integration within Trees and Scaling up from Sample Trees to Entire Forest Stands, *Trees*, 18, 529–546, <https://doi.org/10.1007/s00468-004-0339-6>, 2004.
- Čermák, J., Nadezhkina, N., Meiresonne, L., and Ceulemans, R.: Scots Pine Root Distribution Derived from Radial Sap Flow Patterns in Stems of Large Leaning Trees, *Plant and Soil*, 305, 61–75, <https://doi.org/10.1007/s11104-007-9433-z>, 2008.
- 355 Dansgaard, W.: Stable Isotopes in Precipitation, *Tellus A: Dynamic Meteorology and Oceanography*, 16, 436–468, <https://doi.org/10.3402/tellusa.v16i4.8993>, 1964.
- Dawson, T. E.: Fog in the California Redwood Forest: Ecosystem Inputs and Use by Plants, *Oecologia*, 117, 476–485, <https://doi.org/10.1007/s004420050683>, 1998.
- 360 Dawson, T. E. and Ehleringer, J. R.: Streamside Trees That Do Not Use Stream Water, *Nature*, 350, 335–337, <https://doi.org/10.1038/350335a0>, 1991.
- De Deurwaerder, H. P. T., Visser, M. D., Detto, M., Boeckx, P., Meunier, F., Kuehnhammer, K., Magh, R.-K., Marshall, J. D., Wang, L., Zhao, L., and Verbeeck, H.: Causes and Consequences of Pronounced Variation in the Isotope Composition of Plant Xylem Water, *Biogeosciences*, 17, 4853–4870, <https://doi.org/10.5194/bg-17-4853-2020>, 2020.
- 365 de Jong van Lier, Q., van Dam, J. C., Metselaar, K., de Jong, R., and Duijnsveld, W. H. M.: Macroscopic Root Water Uptake Distribution Using a Matrix Flux Potential Approach, *Vadose Zone Journal*, 7, 1065–1078, <https://doi.org/10.2136/vzj2007.0083>, 2008.
- Dubbert, M., Cuntz, M., Piayda, A., and Werner, C.: Oxygen Isotope Signatures of Transpired Water Vapor: The Role of Isotopic Non-Steady-State Transpiration under Natural Conditions, *New Phytologist*, 203, 1242–1252, <https://doi.org/10.1111/nph.12878>, 2014.
- Dubbert, M., Couvreur, V., Kübert, A., and Werner, C.: Plant Water Uptake Modelling: Added Value of Cross-disciplinary Approaches, *Plant Biology*, 25, 32–42, <https://doi.org/10.1111/plb.13478>, 2023.
- 370 Ehleringer, J. R. and Dawson, T. E.: Water Uptake by Plants: Perspectives from Stable Isotope Composition, *Plant, Cell and Environment*, 15, 1073–1082, <https://doi.org/10.1111/j.1365-3040.1992.tb01657.x>, 1992.
- Fabiani, G., Penna, D., Barbeta, A., and Klaus, J.: Sapwood and Heartwood Are Not Isolated Compartments: Consequences for Isotope Ecohydrology, *Ecohydrology*, <https://doi.org/10.1002/eco.2478>, 2022.
- 375 Feddes, R. A., Kowalik, P., Kolinska-Malinka, K., and Zaradny, H.: Simulation of Field Water Uptake by Plants Using a Soil Water Dependent Root Extraction Function, *Journal of Hydrology*, 31, 13–26, [https://doi.org/10.1016/0022-1694\(76\)90017-2](https://doi.org/10.1016/0022-1694(76)90017-2), 1976.



- Gaines, K. P., Meinzer, F. C., Duffy, C. J., Thomas, E. M., and Eissenstat, D. M.: Rapid Tree Water Transport and Residence Times in a Pennsylvania Catchment: Rapid Tree Water Transport and Residence Times, *Ecohydrology*, 9, 1554–1565, <https://doi.org/10.1002/eco.1747>, 2016.
- 380 Gebauer, T., Horna, V., and Leuschner, C.: Variability in Radial Sap Flux Density Patterns and Sapwood Area among Seven Co-Occurring Temperate Broad-Leaved Tree Species, *Tree Physiology*, 28, 1821–1830, <https://doi.org/10.1093/treephys/28.12.1821>, 2008.
- Geißler, K., Heblack, J., Uugulu, S., Wanke, H., and Blaum, N.: Partitioning of Water Between Differently Sized Shrubs and Potential Groundwater Recharge in a Semi-arid Savanna in Namibia, *Frontiers in Plant Science*, 10, 1411, <https://doi.org/10.3389/fpls.2019.01411>, 2019.
- 385 Gessler, A., Bächli, L., Rouholahnejad Freund, E., Treydte, K., Schaub, M., Haeni, M., Weiler, M., Seeger, S., Marshall, J., Hug, C., Zweifel, R., Hagedorn, F., Rigling, A., Saurer, M., and Meusburger, K.: Drought Reduces Water Uptake in Beech from the Drying Topsoil, but No Compensatory Uptake Occurs from Deeper Soil Layers, *New Phytologist*, 233, 194–206, <https://doi.org/10.1111/nph.17767>, 2022.
- Granier, A.: Une Nouvelle Méthode Pour La Mesure Du Flux de Sève Brute Dans Le Tronc Des Arbres, *Annales des Sciences Forestières*, 42, 193–200, <https://doi.org/10.1051/forest:19850204>, 1985.
- 390 Harvey, R. B.: Tracing the Transpiration Stream with Dyes, *American Journal of Botany*, 17, 657–661, <https://doi.org/10.1002/j.1537-2197.1930.tb04911.x>, 1930.
- Hayes, L.: Review Article The Current Use of TIROS-N Series of Meteorological Satellites for Land-Cover Studies, *International Journal of Remote Sensing*, 6, 35–45, <https://doi.org/10.1080/01431168508948422>, 1985.
- James, S., Meinzer, F., Goldstein, G., Woodruff, D., Jones, T., Restom, T., Mejia, M., Clearwater, M., and Campanello, P.: Axial and Radial
- 395 Water Transport and Internal Water Storage in Tropical Forest Canopy Trees, *Oecologia*, 134, 37–45, <https://doi.org/10.1007/s00442-002-1080-8>, 2003.
- Jarvis, N.: A Simple Empirical Model of Root Water Uptake, *Journal of Hydrology*, 107, 57–72, [https://doi.org/10.1016/0022-1694\(89\)90050-4](https://doi.org/10.1016/0022-1694(89)90050-4), 1989.
- Jefferis, G.: Readbitmap: Simple Unified Interface to Read Bitmap Images (BMP, JPEG, PNG, TIFF), <https://CRAN.R-project.org/package=readbitmap>, 2018.
- 400 Kahmen, A., Buser, T., Hoch, G., Grun, G., and Dietrich, L.: Dynamic 2H Irrigation Pulse Labelling Reveals Rapid Infiltration and Mixing of Precipitation in the Soil and Species-specific Water Uptake Depths of Trees in a Temperate Forest, *Ecohydrology*, 14, <https://doi.org/10.1002/eco.2322>, 2021.
- Kalma, S. J., Thorburn, P. J., and Dunn, G. M.: A Comparison of Heat Pulse and Deuterium Tracing Techniques for Estimating Sap Flow in
- 405 *Eucalyptus Grandis* Trees, *Tree Physiology*, 18, 697–705, <https://doi.org/10.1093/treephys/18.10.697>, 1998.
- Knighton, J., Kuppel, S., Smith, A., Soulsby, C., Sprenger, M., and Tetzlaff, D.: Using Isotopes to Incorporate Tree Water Storage and Mixing Dynamics into a Distributed Ecohydrologic Modelling Framework, *Ecohydrology*, 13, <https://doi.org/10.1002/eco.2201>, 2020.
- Koeniger, P., Marshall, J. D., Link, T., and Mulch, A.: An Inexpensive, Fast, and Reliable Method for Vacuum Extraction of Soil and Plant Water for Stable Isotope Analyses by Mass Spectrometry: Vacuum Extraction of Soil and Plant Water for Stable Isotope Analyses, *Rapid*
- 410 *Communications in Mass Spectrometry*, 25, 3041–3048, <https://doi.org/10.1002/rcm.5198>, 2011.
- Kühnhammer, K., Dahlmann, A., Iraheta, A., Gerchow, M., Birkel, C., Marshall, J. D., and Beyer, M.: Continuous in Situ Measurements of Water Stable Isotopes in Soils, Tree Trunk and Root Xylem: Field Approval, *Rapid Communications in Mass Spectrometry*, 36, <https://doi.org/10.1002/rcm.9232>, 2022.



- Kulmatiski, A. and Forero, L. E.: Bagging: A Cheaper, Faster, Non-Destructive Transpiration Water Sampling Method for Tracer Studies, *Plant and Soil*, 462, 603–611, <https://doi.org/10.1007/s11104-021-04844-w>, 2021.
- 415 Kuppel, S., Tetzlaff, D., Maneta, M. P., and Soulsby, C.: ECH2O-iso-iso 1.0: Water Isotopes and Age Tracking in a Process-Based, Distributed Ecohydrological Model, *Geoscientific Model Development*, 11, 3045–3069, <https://doi.org/10.5194/gmd-11-3045-2018>, 2018.
- Landgraf, J., Tetzlaff, D., Dubbert, M., Dubbert, D., Smith, A., and Soulsby, C.: Xylem Water in Riparian Willow Trees (*Salix Alba*) Reveals Shallow Sources of Root Water Uptake by in Situ Monitoring of Stable Water Isotopes, *Hydrology and Earth System Sciences*, 26, 2073–2092, <https://doi.org/10.5194/hess-26-2073-2022>, 2022.
- 420 Lubczynski, M. W., Chavarro-Rincon, D. C., and Rossiter, D. G.: Conductive Sapwood Area Prediction from Stem and Canopy Areas- Allometric Equations of Kalahari Trees, Botswana, *Ecohydrology*, 10, e1856, <https://doi.org/10.1002/eco.1856>, 2017.
- Magh, R.-K., Eiferle, C., Burzlaff, T., Dannenmann, M., Rennenberg, H., and Dubbert, M.: Competition for Water Rather than Facilitation in Mixed Beech-Fir Forests after Drying-Wetting Cycle, *Journal of Hydrology*, 587, 124 944, <https://doi.org/10.1016/j.jhydrol.2020.124944>, 2020.
- 425 Marshall, D. C.: Measurement of Sap Flow in Conifers by Heat Transport., *Plant Physiology*, 33, 385–396, <https://doi.org/10.1104/pp.33.6.385>, 1958.
- Marshall, J. D., Cuntz, M., Beyer, M., Dubbert, M., and Kuehnhammer, K.: Borehole Equilibration: Testing a New Method to Monitor the Isotopic Composition of Tree Xylem Water in Situ, *Frontiers in Plant Science*, 11, <https://www.frontiersin.org/articles/10.3389/fpls.2020.00358>, 2020.
- 430 Mathiesen, A.: Die Geschwindigkeit und der Verlauf des Transpirationsstromes bei der Birke, *Kungl. Skogshögskolans skrifter*, pp. 10–24, <http://urn.kb.se/resolve?urn=urn:nbn:se:slu:epsilon-e-948>, 1951.
- McJannet, D., Fitch, P., Disher, M., and Wallace, J.: Measurements of Transpiration in Four Tropical Rainforest Types of North Queensland, Australia, *Hydrological Processes*, 21, 3549–3564, <https://doi.org/10.1002/hyp.6576>, 2007.
- 435 Meinzer, F. C., Brooks, J. R., Domec, J.-C., Gartner, B. L., Warren, J. M., Woodruff, D. R., Bible, K., and Shaw, D. C.: Dynamics of Water Transport and Storage in Conifers Studied with Deuterium and Heat Tracing Techniques, *Plant, Cell and Environment*, 29, 105–114, <https://doi.org/10.1111/j.1365-3040.2005.01404.x>, 2006.
- Mennekes, D., Rinderer, M., Seeger, S., and Orlowski, N.: Ecohydrological Travel Times Derived from in Situ Stable Water Isotope Measurements in Trees during a Semi-Controlled Pot Experiment, *Hydrology and Earth System Sciences*, 25, 4513–4530, <https://doi.org/10.5194/hess-25-4513-2021>, 2021.
- 440 Millar, C., Janzen, K., Nehemy, M. F., Koehler, G., Hervé-Fernández, P., Wang, H., Orlowski, N., Barbeta, A., and McDonnell, J. J.: On the Urgent Need for Standardization in Isotope-based Ecohydrological Investigations, *Hydrological Processes*, 36, <https://doi.org/10.1002/hyp.14698>, 2022.
- Müller, D.: Arbeitsteilung Im Buchenholz, *Physiologia Plantarum*, 2, 297–299, <https://doi.org/10.1111/j.1399-3054.1949.tb07654.x>, 1949.
- 445 Parnell, A. C., Phillips, D. L., Bearhop, S., Semmens, B. X., Ward, E. J., Moore, J. W., Jackson, A. L., Grey, J., Kelly, D. J., and Inger, R.: Bayesian Stable Isotope Mixing Models: BAYESIAN STABLE ISOTOPE MIXING MODELS, *Environmetrics*, pp. n/a–n/a, <https://doi.org/10.1002/env.2221>, 2013.
- RCoreTeam: R: A Language and Environment for Statistical Computing, R Foundation for Statistical Computing, <https://www.R-project.org/>, 2022.
- 450 Rothfuss, Y. and Javaux, M.: Reviews and Syntheses: Isotopic Approaches to Quantify Root Water Uptake: A Review and Comparison of Methods, *Biogeosciences*, 14, 2199–2224, <https://doi.org/10.5194/bg-14-2199-2017>, 2017.



- Rozanski, K., Araguás-Araguás, L., and Gonfiantini, R.: Isotopic Patterns in Modern Global Precipitation, in: Geophysical Monograph Series, edited by Swart, P. K., Lohmann, K. C., Mckenzie, J., and Savin, S., pp. 1–36, American Geophysical Union, Washington, D. C., <https://doi.org/10.1029/GM078p0001>, 1993.
- 455 Schneider, C. A., Rasband, W. S., and Eliceiri, K. W.: NIH Image to ImageJ: 25 Years of Image Analysis, *Nature Methods*, 9, 671–675, <https://doi.org/10.1038/nmeth.2089>, 2012.
- Schwendenmann, L., Dierick, D., Kohler, M., and Holscher, D.: Can Deuterium Tracing Be Used for Reliably Estimating Water Use of Tropical Trees and Bamboo?, *Tree Physiology*, 30, 886–900, <https://doi.org/10.1093/treephys/tpq045>, 2010.
- Seeger, S. and Weiler, M.: Temporal Dynamics of Tree Xylem Water Isotopes: In Situ Monitoring and Modeling, *Biogeosciences*, 18, 4603–4627, <https://doi.org/10.5194/bg-18-4603-2021>, 2021.
- 460 Smith, A., Tetzlaff, D., Landgraf, J., Dubbert, M., and Soulsby, C.: Modelling Temporal Variability of in Situ Soil Water and Vegetation Isotopes Reveals Ecohydrological Couplings in a Riparian Willow Plot, *Biogeosciences*, 19, 2465–2485, <https://doi.org/10.5194/bg-19-2465-2022>, 2022.
- Snelgrove, J. R., Buttle, J. M., Kohn, M. J., and Tetzlaff, D.: Co-Evolution of Xylem Water and Soil Water Stable Isotopic Composition in a Northern Mixed Forest Biome, *Hydrology and Earth System Sciences*, 25, 2169–2186, <https://doi.org/10.5194/hess-25-2169-2021>, 2021.
- 465 Steppe, K. and Lemeur, R.: Effects of Ring-Porous and Diffuse-Porous Stem Wood Anatomy on the Hydraulic Parameters Used in a Water Flow and Storage Model, *Tree Physiology*, 27, 43–52, <https://doi.org/10.1093/treephys/27.1.43>, 2007.
- Thorburn, P. J. and Ehleringer, J. R.: Root Water Uptake of Field-Growing Plants Indicated by Measurements of Natural-Abundance Deuterium, *Plant and Soil*, 177, 225–233, <https://doi.org/10.1007/BF00010129>, 1995.
- 470 Thorburn, P. J., Walker, G. R., and Brunel, J.-P.: Extraction of Water from Eucalyptus Trees for Analysis of Deuterium and Oxygen-18: Laboratory and Field Techniques, *Plant, Cell and Environment*, 16, 269–277, <https://doi.org/10.1111/j.1365-3040.1993.tb00869.x>, 1993.
- Tucker, C. J.: Red and Photographic Infrared Linear Combinations for Monitoring Vegetation, *Remote Sensing of Environment*, 8, 127–150, [https://doi.org/10.1016/0034-4257\(79\)90013-0](https://doi.org/10.1016/0034-4257(79)90013-0), 1979.
- 475 Umebayashi, T., Utsumi, Y., Koga, S., Inoue, S., Shiiba, Y., Arakawa, K., Matsumura, J., and Oda, K.: Optimal Conditions for Visualizing Water-Conducting Pathways in a Living Tree by the Dye Injection Method, *Tree Physiology*, 27, 993–999, <https://doi.org/10.1093/treephys/27.7.993>, 2007.
- Volkman, T. H. M., Haberer, K., Gessler, A., and Weiler, M.: High-resolution Isotope Measurements Resolve Rapid Ecohydrological Dynamics at the Soil–Plant Interface, *New Phytologist*, 210, 839–849, <https://doi.org/10.1111/nph.13868>, 2016a.
- Volkman, T. H. M., Kühnhammer, K., Herbstritt, B., Gessler, A., and Weiler, M.: A Method for *in Situ* Monitoring of the Isotope Composition of Tree Xylem Water Using Laser Spectroscopy: *In Situ* Monitoring of Xylem Water Isotopes, *Plant, Cell & Environment*, 39, 2055–2063, <https://doi.org/10.1111/pce.12725>, 2016b.
- 480 Zuecco, G., Amin, A., Frentress, J., Engel, M., Marchina, C., Anfodillo, T., Borga, M., Carraro, V., Scandellari, F., Tagliavini, M., Zanutelli, D., Comiti, F., and Penna, D.: A Comparative Study of Plant Water Extraction Methods for Isotopic Analyses: Scholander-type Pressure Chamber vs. Cryogenic Vacuum Distillation, *Hydrology and Earth System Sciences*, 26, 3673–3689, <https://doi.org/10.5194/hess-26-3673-2022>, 2022.
- 485